

University of Wollongong

Research Online

Faculty of Science, Medicine and Health -
Papers: Part B

Faculty of Science, Medicine and Health

1-1-2019

Proton supplier role of binuclear gold complexes in promoting hydrofunctionalisation of nonactivated alkenes

Maryam Asgari
Islamic Azad University

Christopher J. T Hyland
University of Wollongong, chrhyl@uow.edu.au

A. Stephen K. Hashmi
Heidelberg University

Brian F. Yates
University of Tasmania

Alireza Ariafard
Islamic Azad University, University of Tasmania, Alireza.Ariafard@utas.edu.au

Follow this and additional works at: <https://ro.uow.edu.au/smhpapers1>

Publication Details Citation

Asgari, M., Hyland, C. J., Hashmi, A. K., Yates, B. F., & Ariafard, A. (2019). Proton supplier role of binuclear gold complexes in promoting hydrofunctionalisation of nonactivated alkenes. Faculty of Science, Medicine and Health - Papers: Part B. Retrieved from <https://ro.uow.edu.au/smhpapers1/608>

Research Online is the open access institutional repository for the University of Wollongong. For further information contact the UOW Library: research-pubs@uow.edu.au

Proton supplier role of binuclear gold complexes in promoting hydrofunctionalisation of nonactivated alkenes

Abstract

Density functional theory (DFT) was used to investigate PR_3AuOTf -catalyzed hydrofunctionalisation of nonactivated alkenes using acetic acid and phenol where $\text{OTf} = \text{triflate} (\text{CF}_3\text{SO}_3^-)$. The gold(I) complex itself is found to be unlikely to operate as the π -activator due to its relatively low electrophilicity. Instead, the concurrent coordination of two gold(I) complexes to a nucleophile (PhOH or AcOH) enhances the acidity of the latter's proton and causes the ensuing binuclear complex to serve as a strong proton supplier for activating the alkene π -bonds. Alternatively, the binuclear complex is also susceptible to produce a hidden HOTf . This hidden acid is accessible for hydrofunctionalization to occur but it is not in sufficient concentration to decompose the final product.

Publication Details

Asgari, M., Hyland, C. J. T., Hashmi, A. K., Yates, B. F. & Ariaferd, A. (2019). Proton supplier role of binuclear gold complexes in promoting hydrofunctionalisation of nonactivated alkenes. *Catalysis Science and Technology*, 9 (6), 1420-1426.

Proton Supplier Role of Binuclear Gold Complexes in Promoting Hydrofunctionalisation of nonactivated Alkenes

Maryam Asgari,^a Christopher Hyland,^b A. Stephen K. Hashmi,^c Brian F. Yates,^d Alireza Ariafarid^{*,a,d}

^aDepartment of Chemistry, Central Tehran Branch, Islamic Azad University, Shahrak Gharb, Tehran, Iran

^bSchool of Chemistry and Molecular Bioscience, University of Wollongong, Wollongong, New South Wales 2522, Australia

^cOrganisch-Chemisches Institut, Heidelberg University, Im Neuenheimer Feld 270, 69120 Heidelberg, Germany

^dSchool of Natural Sciences (Chemistry), University of Tasmania, Private Bag 75, Hobart TAS 7001, Australia

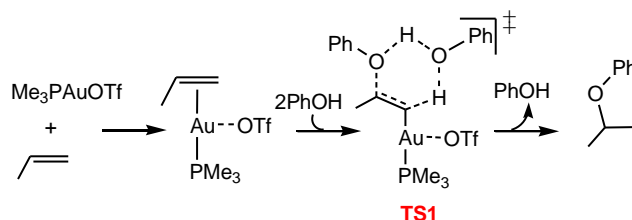
KEYWORDS. Alkene hydrofunctionalization, gold catalysis, Brønsted acid catalysis, LBA activation mode, Density functional theory (DFT)

Density functional theory (DFT) was used to investigate PR_3AuOTf -catalyzed hydrofunctionalisation of nonactivated alkenes using acetic acid and phenol where $\text{OTf} = \text{triflate} (\text{CF}_3\text{SO}_3^-)$. The gold(I) complex itself is found to be unlikely to operate as the π -activator due to its relatively low electrophilicity. Instead, the concurrent coordination of two gold(I) complexes to a nucleophile (PhOH or AcOH) enhances the acidity of the latter's proton and causes the ensuing binuclear complex to serve as a strong proton supplier for activating the alkene π -bonds. Alternatively, the binuclear complex is also susceptible to produce a hidden HOTf. This hidden acid is accessible for hydrofunctionalization to occur but it is not in sufficient concentration to decompose the final product.

Introduction

Brønsted- and Lewis-acid-catalyzed hydrofunctionalizations of unactivated alkenes have attracted considerable attention as methods for the synthesis of highly functionalized molecules which have found numerous applications in pharmaceuticals and agrochemicals.¹⁻³ Although understanding the mechanism of these reactions is fundamental in designing more efficient catalytic processes, investigations in this regard are still scarce. For instance, it is not very clear yet whether Lewis-acids are directly involved in activating the π -bond of alkenes⁴ or if they serve as Brønsted acid generators through reaction with nucleophiles and thus the ensuing protons catalyze the reaction.^{2^{d,5}} As the very first example in the context of Lewis-acid catalyzed hydrofunctionalization, He and co-workers explored HOTf- and PPh_3AuOTf -catalyzed addition of phenols and carboxylic acids to nonactivated alkenes in toluene.⁶ They found that while HOTf promotes the reaction over the temperature range from 25 (for phenols) to 50 °C (for carboxylic acids), the reaction with the gold catalyst needs a higher temperature (85 °C). This result led them to suggest that HOTf is more reactive than PPh_3AuOTf .^{6^{b,7}} By making thorough observations (*vide infra*), they proposed that the gold center itself should be responsible for activating the π -bond and the reaction is not likely to be catalyzed by an *in situ* generated Brønsted acid. For example, they found that certain functional groups were compatible with the gold catalyst but decomposed in the presence of HOTf. They also reported that no reaction took place when an alkene is added to a mixture of PPh_3AuOTf and phenol at room temperature over two days. The functionalized ether products were reported to undergo decomposition at high temperature (85 °C) in the presence of the HOTf catalyst, whereas the decomposition does not occur when PPh_3AuOTf is used as the catalyst.^{6^b}

Subsequently, Ujaque et al. published two distinct theoretical studies associated with the mechanism of these reactions albeit without considering the entropy effects.⁸ They proposed that the hydroaryloxylation should proceed via transition structure **TS1** (Scheme 1) by which the nucleophilic attack and the proton transfer take place simultaneously.⁹ However, our own calculations, which do consider entropic effects, demonstrate that this transition structure should be energetically inaccessible ($\Delta G^\ddagger = 53.0$ kcal/mol). This result is consistent with our previous studies which signified that the gold(I) complexes are not electrophilic enough to activate carbon-carbon double bonds toward some types of nucleophilic attack.¹⁰ In light of this, we need to turn our attention to an alternative mechanism by which the nucleophilic addition is facilitated by a stronger electrophile such as a proton.



Scheme 1. Mechanism proposed by Ujaque et al. which were calculated by us to need an activation Gibbs energy as high as 53.0 kcal/mol

Recently, it was discovered that triflate metal complexes in the presence of nucleophiles readily generates HOTf.¹¹ In such a case, *in situ* generated HOTf was proposed to serve as the real catalyst for hydrofunctionalization of alkenes. The question raised at this stage is whether HOTf can indeed be generated by PPh_3AuOTf in the presence of a nucleophile. If so, why doesn't the *in situ* generated HOTf behave similarly to the HOTf catalyst, as demonstrated

by He et al.? What is the mechanism for HOTf generation? Herein we provide some additional clarity with regards to these contradicting results for the PPh_3AuOTf - and HOTf-catalyzed hydroaryloxylation and hydroacetoxylation of nonactivated alkenes.

Results and discussion

We commence our discussion by investigating a HOTf-catalyzed hydroacetoxylation of propene. The mechanism of HOTf-catalyzed phenol and amine addition to simple alkenes has been separately reported by Li and Ujaque et al.^{8b,12} They both proposed that the most favorable mechanism should involve a cyclic concerted transition structure, yielding a *syn*-product (pathway A in Fig. 1). In contrast, we found that, for this kind of transformation, an alternative mechanism (pathway B) is more favorable (Fig. 1). Our proposed mechanism, which gives an *anti*-product, starts with formation of intermediate **1** via concerted 1,2 addition of H-OTf to the carbon-carbon double bond, followed by an $\text{S}_{\text{N}}2$ reaction between the nucleophile and intermediate **1**.¹³ The calculations for hydroacetoxylation of propene show that **TS3** is about 5.6 kcal/mol lower in energy than **TS2**, implying more favorability of pathway B. Further calculations at the M06-D3-CPCM level support this finding and indicates that pathway B is favored over pathway A by 4.8 kcal/mol (Fig. S1). These results are consistent with an experimental study concerning addition of acetic acid to 2-butene in which the authors reported a stepwise mechanism and not concerted proceeded via a tight-ion pair similar to intermediate **1**.¹⁴

The $\text{S}_{\text{N}}2$ process assisted by a second HOAc (via **TS4**) is found to be 3.9 kcal/mol lower in energy than the non-assisted one (via **TS5**); the strong hydrogen bonding interactions created by the second HOAc in **TS4** render this transition structure lower in energy than **TS5**. The $\text{S}_{\text{N}}2$ reaction can also be assisted by adventitious water or another molecule of HOTf, both of which are computed to be slightly less favorable (Fig. S1 and S2).

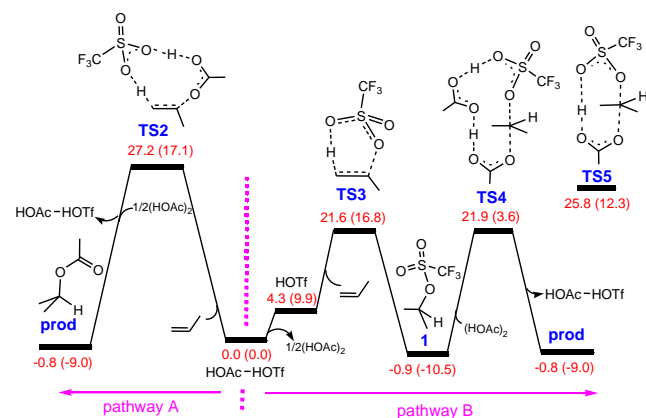


Fig. 1 Energy profile for HOTf-catalyzed hydroacetoxylation of propene from pathways A and B calculated at the B3LYP-D3-CPCM/BS2//B3LYP-CPCM/BS1 level of theory in toluene. Free energies (potential energies) are given in kcal/mol

Pathway B for hydroaryloxylation of propene is also computed to be favored by 4.5 kcal/mol over pathway A (Fig. S3). The transition structure **TS3** for hydroaryloxylation with $\Delta G^\ddagger = 18.6$ kcal/mol (Fig. S3) is lower in energy than that for hydroacetoxylation with $\Delta G^\ddagger = 21.6$ kcal/mol (Fig. 1). This finding can be explained in terms of the weaker hydrogen bond interaction in HOTf-HOTf and PhOH-HOTf

than in HOAc-HOTf; the binding free energies in dimers HOAc-HOTf, HOAc-HOAc, HOTf-HOTf, PhOH-HOTf and PhOH-PhOH are calculated to be -5.9 , -3.3 , -2.6 , 0.0 and 3.3 kcal/mol, respectively. The weaker hydrogen bonding in HOTf-HOTf and PhOH-HOTf allows HOTf to be more available to participate in the catalytic cycle. This finding may explain why the hydroaryloxylation experimentally needed a lower temperature (*vide supra*).

Let us now inspect the PMe_3AuOTf -catalyzed hydroacetoxylation of propene. The PMe_3AuOTf complex is calculated to be the catalyst resting state; other possible complexes are less stable or have a similar stability. The high stability of outer sphere complexes **3** and **5** compared to the cationic complexes **4** and **6** indicates the importance of cation-anion interactions in these systems, which in turn force the OTf⁻ anion to always be in the vicinity of the cationic gold complex.

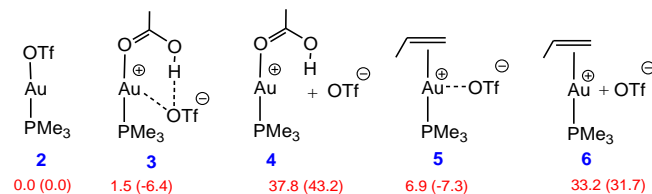


Fig. 2 Relative energies for structures **2**, **3**, **4**, **5** and **6**. Free energies (potential energies) are given in kcal/mol.

For the gold-catalyzed reaction, we first explored a mechanism analogous to that proposed by Ujaque et al. (Scheme 1) in which the gold centre itself is responsible for activating the π bond (Fig. 3). As anticipated, the activation barrier for addition of HOAc is extremely high, corroborating the fact that the gold center alone is not able to trigger the hydrofunctionalization. Similarly to **TS1**, the nucleophilic attack and the proton transfer take place concurrently in **TS6**. This result led us to conclude that the gold(I) complex is not electrophilic enough to activate propene in the catalytic cycle and this process should occur by a stronger electrophilic center such as a proton.

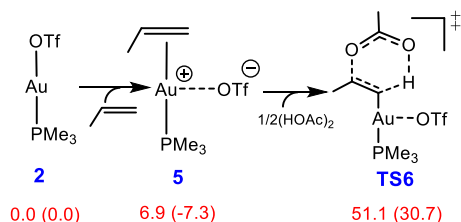


Fig. 3 Mechanism for hydroacetoxylation of propene via six membered cyclic transition structure **TS6** calculated at the B3LYP-D3-CPCM/BS2//B3LYP-CPCM/BS1 level of theory in toluene. Free energies (potential energies) are given in kcal/mol.

It is well documented that coordination of nucleophiles to Lewis acids increases the acidity of the former, allowing them to serve as a proton supplier.¹⁰ This combination indeed creates a catalyst, which is capable of operating via a Lewis acid-assisted Brønsted acid (LBA) activation mode.¹⁵ As mentioned earlier, the ensuing proton in the presence of an OTf ligand is thought to be released as HOTf and thus in this case, HOTf should catalyze the reaction. Fig. 4 presents our initial findings concerning the activation of propene via the LBA activation mode. According to this mechanism, coordination of HOAc to gold(I) is surmised to initiate the reaction. Intermediate **3** is a branching point for two competitive pathways

(Fig. 4). Both pathways (C and D) entail formation of the key intermediate **1**. In pathway C, propene itself acts as a base and abstracts a proton from HOAc-bound gold complex **3** via **TS7**, resulting in concurrent addition of OTf and hydrogen across the C=C bond of propene. This pathway features a concerted formation of **1**. In pathway D, formation of intermediate **1** takes place via a stepwise mechanism: the [OTf]⁻ counter ion deprotonates complex **3** to afford HOTf and then the resultant acid is added to the alkene via **TS3**. It appears from comparison of Fig. 3 and 4 that the propene activation via the gold-assisted Brønsted acid system has a much lower energy barrier than that occurring by the gold center itself. This result emphasizes the necessity of the LBA catalyst for propene activation. However, the computed energy barriers still seem too high for the reaction to proceed under experimental conditions (85 °C for 15 h in toluene). The high barriers can be explained in terms of the relatively low acidity of the proton in complex **3**. Indeed, a gold(I) center alone does not provide sufficient enhancement of the acidity of the proton, as evident from the high endergonicity for transformations **3** → HOTf + **7** ($\Delta G = 20.4$ kcal/mol) and **3** + propene → **1** + **7** ($\Delta G = 15.2$ kcal/mol). In such a case, a more powerful LBA catalyst is expected to be responsible for conducting the reaction.

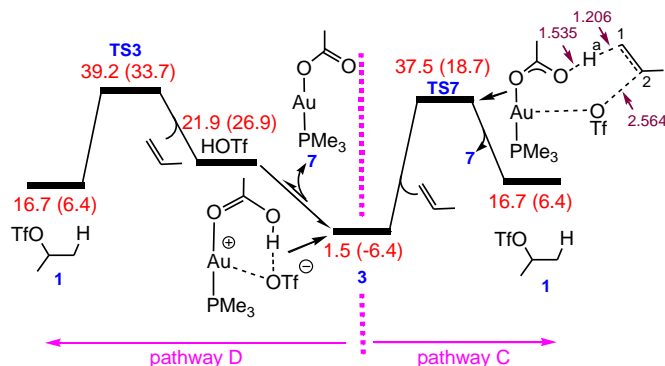


Fig. 4 Energy profile for formation of **1** from complex **3** calculated at the B3LYP-D3-CPCM/BS2//B3LYP-CPCM/BS1 level of theory in toluene. Free energies (potential energies) are given in kcal/mol.

Recently, Tamai et al. reported gold(I)-catalyzed hydrothiolation of alkenes and identified formation of a tetranuclear gold complex $[L_4Au_4(\mu\text{-SPh})_2]^{2+}$ during the course of this process.¹⁶ In this tetranuclear gold complex, two $[(LAu)_2(\mu\text{-SPh})]^+$ species are bonded together via an aurophilic interaction. The formation of such a complex may suggest that the hydrothiolation likely proceed via a binuclear mechanism. This fascinating finding prompted us to investigate possibility of a binuclear mechanism for the hydroacetoxylation reaction. To our delight, our calculations validated this hypothesis and disclosed that if binuclear complex **9** is formed, the condition for better activation of propene is met. This binuclear complex is calculated to lie only 5.6 kcal/mol above the resting state **3** (Fig. 5a), implying that its formation should be thermodynamically feasible. In **9**, one of the OTf anions is stabilized by electrostatic interaction with both gold centres. The electrostatic nature of this interaction is supported by the very small values for the Wiberg bond index (WBI) between the gold centers and the oxygen atoms of the OTf (Fig. 5b). The shorter Au¹-O³ and Au²-O³ distances in this binuclear complex suggests that the effect of the O³ atom on the stability of the outer-sphere binuclear complex is

more significant than the other two oxygens. The hydrogen bonding between the second OTf and the coordinated HOAc also plays an important role in the stability of complex **9**. The long distance of 3.560 Å and a small WBI between Au¹ and Au² (0.017) implies a very negligible covalent interaction between these two metal centers.

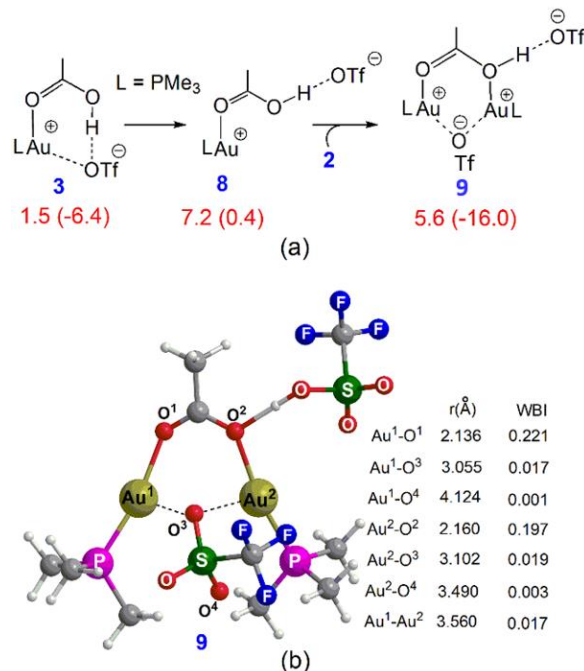


Fig. 5 (a) Relative energies for intermediates **3**, **8** and **9** where L = PMe₃. Free energies (potential energies) are given in kcal/mol. (b) Optimized geometry for **9** along with selective distances and Wiberg bond indices (WBIs).

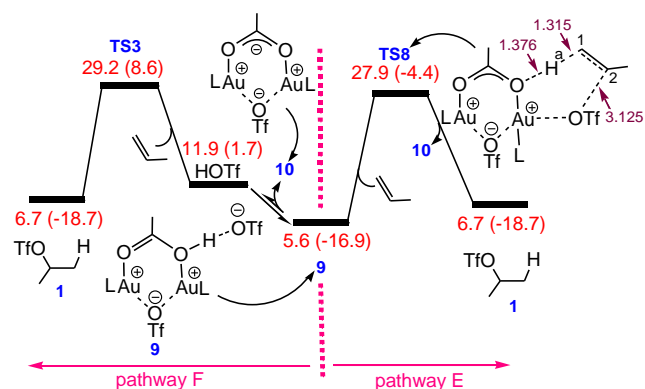


Fig. 6 Energy profile for formation of **1** from binuclear complex **9** calculated at the B3LYP-D3-CPCM/BS2//B3LYP-CPCM/BS1 level of theory in toluene where L = PMe₃. Free energies (potential energies) are given in kcal/mol.

Our calculations show that when the binuclear complex **9** is used as the LBA catalyst, the free energy of activation is lowered by 10 kcal/mol (Fig. 6). This reduction in activation energy is due to the increased acidity of the proton in **9** compared to that **3**. This assertion is supported by the relatively low endergonicity for transformations **9** → HOTf + **10** ($\Delta G = 6.3$ kcal/mol) and **9** + propene → **1** + **10** ($\Delta G = 1.1$ kcal/mol). Structural comparison between **TS7** and

TS8 also confirms the above claim; **TS8** has a shorter O-H^a distance and longer C¹-H^a and C²-OTf distances than those in **TS7** (Fig. 4 and 6), indicating that **TS8** is an early transition structure owing to the higher acidity of the proton in **9**.

To further assess the validity of the results obtained from the B3LYP-D3-CPCM/BS2//B3LYP-CPCM/BS1 level, single-point energy calculations using M06-D3-CPCM/BS2 and B97D-CPCM/BS2 in toluene were carried out for pathways C-F. Both levels predict that pathways E and F are far more favourable than pathways C and D and activation energies for pathways E and F are comparable (Table S1). The same conclusion was reached when the PMe₃ ligand is replaced with PPh₃, when the structures are optimized by inclusion of dispersion interactions, and when def2-SVP is used instead of LANL2DZ to describe the gold centre (Table S1).

Once the key intermediate **1** is formed, two likely pathways can compete to give the final product (**prod**). Pathway G involves the reaction of **1** with an acetic acid dimer via a S_N2 mechanism, whereas in pathway H, the S_N2 reaction takes place between binuclear complex **10** and intermediate **1** via **TS9**. The calculations at the B3LYP-D3-CPCM/BS2//B3LYP-CPCM/BS1 level of theory predict that pathway G is about 3.8 kcal/mol more favourable than pathway H. In such a case, the calculated overall free energy barrier for hydroacetoxylation of propene is calculated to be 29.4 kcal/mol. This large barrier height explains why the hydrofunctionalization catalyzed by LAuOTf requires more vigorous conditions than that catalysed by HOTf (*vide supra*). It appears from Fig. 7 that formation of **prod** is endergonic by 6.8 kcal/mol. However, this endergonicity is changed to exergonicity if decomposition of complex **10** by HOTf to the LAuOTf precatalyst is taken into account.

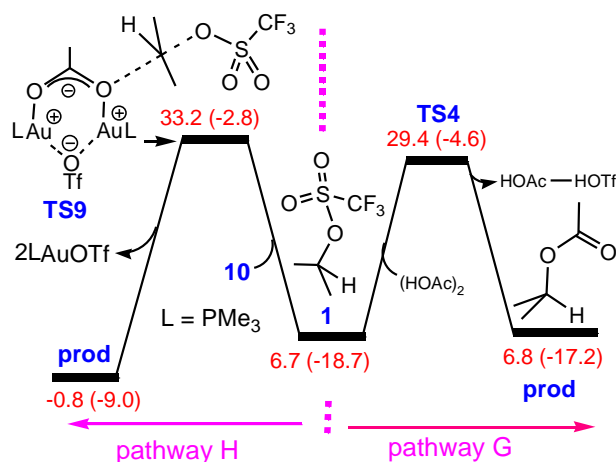
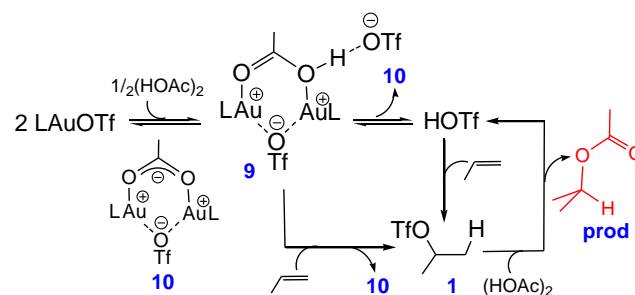


Fig. 7 Energy profile for formation of **prod** from **1** calculated at the B3LYP-D3-CPCM/BS2//B3LYP-CPCM/BS1 level of theory in toluene where L = PMe₃. Free energies (potential energies) are given in kcal/mol.

The detailed catalytic cycle of the gold(I)-catalyzed hydroacetoxylation of propene is summarized in Scheme 2. LAuOTf is computed to be the catalyst resting state.¹⁷ The interaction of two equivalents of LAuOTf (precatalyst) with acetic acid generates the active catalyst **9** in which the proton of the coordinated acid becomes extremely acidic.¹⁸ The active catalyst can be involved in either a concerted reaction with propene to give the key intermediate **1** or a stepwise mechanism to first generate the second active catalyst

HOTf followed by formation of **1** through reaction of the ensuing acid with propene. Finally, treatment of intermediate **1** with acetic acid gives the hydroacetoxylation product (**prod**) and reproduces HOTf. The regeneration of complex **9** easily occurs via interaction of HOTf with the binuclear complex **10**.¹⁹



Scheme 2. Catalytic Cycle Summarizing Our Findings

By analogy, the binuclear complex **9'** is found to be the LBA catalyst for the hydroaryloxylation of alkenes in the presence of LAuOTf (Fig. 8). In this case, pathway F lies 1.9 kcal/mol lower in energy pathway E, suggesting that in situ generated HOTf likely drives the catalytic reaction. Intermediate [(LAu)₂(μ-OPh)]OTf is reminiscent of the tetranuclear gold complex [L₄Au₄(μ-SPh)₂]²⁺, characterized by Tamai et al. during the course of gold(I)-catalyzed hydrothiolation of alkenes. As discussed earlier, this tetranuclear complex is stabilized by an aurophilic interaction between two [(LAu)₂(μ-SPh)]⁺ species. Our calculations show that, although the aurophilic interaction in [L₄Au₄(μ-SPh)₂]²⁺ with ΔE = 10.7 kcal/mol is significant, that is not the case for [L₄Au₄(μ-OPh)₂]²⁺; no local minimum exists for [L₄Au₄(μ-OPh)₂]²⁺ at the B3LYP-CPCM/BS1 level. This implies that the stability of the tetranuclear gold complexes depends on the nature of the bridging ligand.

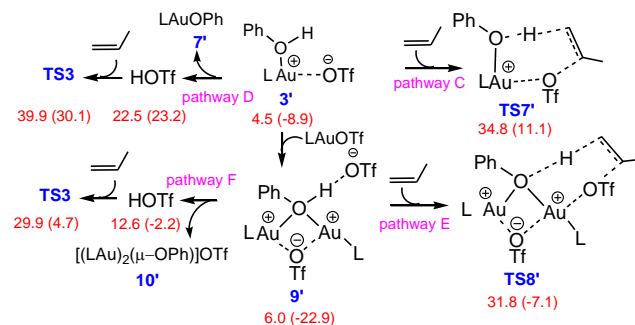


Fig. 8 Mechanism for LAuOTf-catalyzed hydroaryloxylation of propene calculated at the B3LYP-D3-CPCM/BS2//B3LYP-CPCM/BS1 level of theory in toluene where L = PMe₃. Free energies (potential energies) are given in kcal/mol.

As mentioned earlier, the functionalized ether products decompose at high temperature (85 °C) in the presence of the HOTf catalyst, whereas the decomposition does not occur when LAuOTf is used as the catalyst. This appears to be in contradiction with the notion that both reactions are catalyzed by HOTf. This inconsistency can be explained in terms of the negligible availability of HOTf in the gold catalysis pathway ('hidden' HOTf). Our calculations predict that the concentration of HOTf in the process initiated by LAuOTf is trivial (as evident from the endergonicity of 11.9 kcal/mol for the transformation 2LAuOTf + ½(HOAc)₂ → HOTf + **10**) and thus the in situ generated acid cannot play any role in the

product decomposition. For example, a possibility for the decomposition is that the product becomes involved in a polymerization reaction. As can be seen from Fig. 9, in the gold catalysis, **1** + propene has a free energy of 13.5 kcal/mol relative to two equivalents of **prod**, causing the transition structure relating to the propagation step to be highly energetic ($\Delta G^\ddagger = 44.2$ kcal/mol). In contrast, the same transition structure in the HOTf catalysis, due to the high concentration of HOTf, lies 12.8 kcal/mol lower in energy, resulting in the polymerization being a more feasible process in this system.

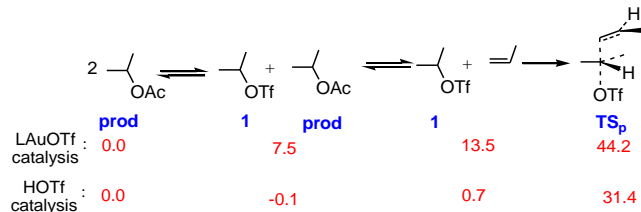


Fig. 9 Relative free energies of key stationary points for polymerization propagation step from **prod** calculated at the B3LYP-D3-CPCM/BS2//B3LYP-CPCM/BS1 level of theory in toluene. Free energies are given in kcal/mol.

Conclusions

In conclusion, clarification of the nature of the catalyst in gold-catalysed alkene hydroaryloxylation and hydroacetoxylation has revealed the true nature of the catalysis to be via a Lewis acid-assisted Brønsted acid mode – either directly employing binuclear **9/9'** or generating triflic acid. This has important implications for gold-catalysed hydrofunctionalisation reactions and similar reactions,²⁰ potentially allowing for the design of well-defined gold-derived LBA catalysts. Furthermore, this understanding could increase the scope of other Brønsted-acid-catalysed hydrofunctionalisation reactions through the in-situ generation of low local concentrations of powerful Brønsted-acids.

Computational methods

Gaussian 09²¹ was used to fully optimize all the structures reported in this paper at the B3LYP level of theory.²² For all the calculations, solvent effects were considered using the CPCM solvation model with toluene as the solvent.²³ The effective-core potential of Hay and Wadt with a double- ξ valence basis set (LANL2DZ) was chosen to describe Au.²⁴ The 6-31G(d) basis set was used for other atoms.²⁵ A polarization function was also added for Au ($\xi_f = 1.050$).²⁶ This basis set combination will be referred to as BS1. Frequency calculations were carried out at the same level of theory as those for the structural optimization. Transition structures were located using the Berny algorithm. Intrinsic reaction coordinate (IRC) calculations were used to confirm the connectivity between transition structures and minima.²⁷ To further refine the energies obtained from the B3LYP-CPCM/BS1 calculations and to consider dispersive interactions,²⁸ we carried out single-point energy calculations using the B3LYP-D3 functional method for all of the structures with a larger basis set (BS2) and the CPCM solvation model. BS2 utilizes the def2-TZVP basis set²⁹ on all atoms. Effective core potentials including scalar relativistic effects were used for the gold atom. To increase the accuracy of the calculations, tight convergence criterion was employed. To validate the accuracy of the B3LYP-D3-CPCM/BS2//B3LYP-CPCM/BS1 calculations in predicting a favored mechanism, the single point calculations were repeated by using the M06-D3-CPCM/BS₂ and B97D-CPCM/BS2 methods.^{30,31} Our calculations for geometry optimizations show that the replacement of LANL2DZ with def2-SVP and B3LYP with B3LYP-D3 insignificantly affect the activation free energies (Table S1). Wiberg bond indices were calculated by natural bond orbital analysis using NBO6 software^{32,33} integrated into Gaussian09.

Conflict of interests

There are no conflicts of interest to declare.

Acknowledgements

We thank the Australian Research Council for financial support (project number DP180100904) and the Australian National Computational Infrastructure and the University of Tasmania for computing resources.

Notes and references

- J. F. Hartwig, in *Organotransition Metal Chemistry*; University Science Books: Sausalito, CA, 2010.
- (a) C. Liu, C. F. Bender, X. Han and R. A. Widenhoefer, *Chem. Commun.*, 2007, 3607; (b) M. Chiarucci and M. Bandini, *Beilstein J. Org. Chem.*, 2013, **9**, 2586; (c) E. M. Barreiro, L. A. Adrio, K. (M.) Hii and J. B. Brazier, *Eur. J. Org. Chem.*, 2013, 1027; (d) N. Hugué and A. M. Echavarren, *Top. Organomet. Chem.*, 2013, **43**, 291; (e) J. S. Yadav, A. Antony, T. S. Rao and B. V. S. Reddy, *J. Organomet. Chem.*, 2011, **696**, 16; (f) S. Antoniotti, S. Poulain-Martini and Duñach, *E. Synlett.*, 2010, **20**, 2973.
- For hydrofunctionalization of alkenes catalyzed by transition metal complexes see: (a) H. Murayama, K. Nagao, H. Ohmiya and M. Sawamura, *Org. Lett.*, 2015, **17**, 2039; (b) M. C. Haibach, C. Guan, D. Y. Wang, B. Li, N. Lease, A. M. Steffens, K. Krogh-Jespersen and A. S. Goldman, *J. Am. Chem. Soc.*, 2013, **135**, 15062; (c) H. Shigehisa, T. Aoki, S. Yamaguchi, N. Shimizu and K. Hiroya, *J. Am. Chem. Soc.*, 2013, **135**, 10306; (d) C. S. Sevov and J. F. Hartwig, *J. Am. Chem. Soc.*, 2013, **135**, 9303; (e) T. Hirai, A. Hamasaki, A. Nakamura and M. Tokunaga, *Org. Lett.*, 2009, **11**, 5510; (f) R. Corberán, S. Marrot, N. Dellus, N. Merceron-Saffon, T. Kato, E. Peris and A. Baceiredo, *Organometallics.*, 2009, **28**, 326; (g) J. Tan, Z. Zhang and Z. Wang, *Org. Biomol. Chem.*, 2008, **6**, 1344; (h) J.-C. Choi, K. Kohno, D. Masuda, H. Yasuda and T. Sakakura, *Chem. Commun.*, 2008, 777.
- For hydrofunctionalization reactions in which the Lewis-acid itself is proposed to directly activate the alkene π -bond toward nucleophiles see: (a) C. F. Bender, T. J. Brown and R. A. Widenhoefer, *Organometallics.*, 2016, **35**, 113; (b) R. L. LaLonde, Jr. W. E. Brenzovich, D. Benitez, E. Tkatchouk, K. Kelley, W. A. Goddard and F. D. Toste, *Chem. Sci.*, 2010, **1**, 226; (c) C. Palo-Nieto, A. Sau and M. C. Galan, *J. Am. Chem. Soc.*, 2017, **139**, 14041; (d) A. Dzudza and T. J. Marks, *Org. Lett.*, 2009, **11**, 1523; (e) G. Kovács, G. Ujaque and A. Lledós, *J. Am. Chem. Soc.*, 2008, **130**, 853.

- 5 For hydrofunctionalization reactions in which Lewis-acid is proposed to act as a mediator for transfer of a proton to alkene see: (a) D. C. Rosenfeld, S. Shekhar, A. Takemiya, M. Utsunomiya and J. F. Hartwig, *Org. Lett.*, 2006, **8**, 4179; (b) J. L. McBee, A. T. Bell and T. D. Tilley, *J. Am. Chem. Soc.*, 2008, **130**, 16562; (c) X. Zhu, G. Li, F. Xu, Y. Zhang, M. Xue and Q. Shen, *Tetrahedron*, 2017, **73**, 1451; (d) M. J. Deka, K. Indukuri, S. Sultana, M. Borah and A. K. Saikia, *J. Org. Chem.*, 2015, **80**, 4349.
- 6 (a) C. Yang and C.-G. He, *J. Am. Chem. Soc.*, 2005, **127**, 6966; (b) Z. Li, J. Zhang, C. Brouwer, C.-G. Yang, N. W. Reich and C. He, *Org. Lett.*, 2006, **8**, 4175.
- 7 For the early view on the role of protons in gold catalysis, see: A. S. K Hashmi, *Catal. Today*, 2007, **122**, 211.
- 8 (a) G. Kovács, A. Lledós and G. Ujaque, *Organometallics*, 2010, **29**, 3252; (b) G. Kovács, A. Lledós and G. Ujaque, *Organometallics*, 2010, **29**, 5919.
- 9 Proton transfer process reported by Ujaque et al. resembles the function of the water clusters as proton shuttles for long distance proton transfer in gold catalysis; for details see: C. M. Krauter, A. S. K. Hashmi M. Pernpointner, *ChemCatChem*, 2010, **2**, 1226.
- 10 (a) T. Mehrabi and A. Ariafard, *Chem. Commun.*, 2016, **52**, 9422 (b) J. Schiebl, M. Rudolph and A. S. K. Hashmi, *Adv. Synth. Catal.*, 2017, **359**, 639.
- 11 (a) M. J.-L. Tschan, C. M. Thomas, H. Strub and J.-F. Carpentier, *Adv. Synth. Catal.*, 2009, **351**, 2496; (b) T. T. Dang, F. Boeck and L. Hintermann, *J. Org. Chem.*, 2011, **76**, 9353; (c) J. Chen, S. K. Goforth, B. A. McKeown and T. B. Gunnoe, *Dalton Trans.*, 2017, **46**, 2884.
- 12 X. Li, S. Ye, C. He and Z.-X. Yu, *Eur. J. Org. Chem.*, 2008, 4296.
- 13 Since a nonpolar solvent (toluene) is utilized in the experimental study, the charge separation of **1** into $\text{CH}_3\text{CHCH}_3^+ + \text{OTf}^-$ is anticipated to be very energy consuming. Our calculations lend support to this claim and indicate that transformation $\mathbf{1} \rightarrow \text{CH}_3\text{CHCH}_3^+ + \text{OTf}^-$ is endergonic by +62.1 kcal/mol. As such, conversion of **1** to **prod** should preferentially take place via a $\text{S}_{\text{N}}2$ process under these conditions – however, an $\text{S}_{\text{N}}1$ should not be excluded in different solvents.
- 14 D. J. Pasto and J. F. Gadberry, *J. Am. Chem. Soc.*, 1978, **100**, 1469.
- 15 H. Yamamoto and K. Futatsugi, *Angew. Chem. Int. Ed.*, 2005, **44**, 1924.
- 16 T. Tamai, K. Fujiwara, S. Higashimae, A. Nomoto and A. Ogawa, *Org. Lett.*, 2016, **18**, 2114.
- 17 Replacement of LAuOTf with LAuOH is expected to inactivate the catalyst toward the mechanism proposed in this study. Our calculations predicate that the reaction between PMe_3AuOH and $0.5(\text{HOAc})_2$ gives $\text{PMe}_3\text{AuOAc} \cdot \text{H}_2\text{O}$ in an exergonic fashion with $\Delta G = -8.2$ kcal/mol. Indeed, the higher basic character of the counter anion in LAuOH than in LAuOTf results in H_2O instead of HOTf being formed during the catalytic reaction which is not acidic enough to protonate the alkenes. It follows that our binuclear mechanism is operative if the counter anion X of the LAuX catalyst is capable of forming a strong acid such as HOTf when the catalyst reacts with the substrate.
- 18 (a) So far, the gold(I)-oxygen interaction has considered to be very weak only: N. Ibrahim, M. H. Vilhelmsen, M. Pernpointner, F. Rominger and A. S. K. Hashmi, *Organometallics*, 2013, **32**, 2576; (b) for the formation of thermodynamically quite stable polynuclear clusters from gold(I) and also weakly binding N-ligands, see: C. Khin, A. S. K. Hashmi and F. Rominger, *Eur. J. Inorg. Chem.*, 2010, 1063
- 19 Another possibility for the hydroacetoxylation to occur is that LAuOAc (**7**) reacts with the alkene complex **5**. Our calculations indicate that this pathway (Fig S6) requires an activation Gibbs energy of 37.2 kcal/mol, which is by 8 kcal/mol higher in energy than our binuclear mechanism (Scheme 2). This sort of mechanism has been already discussed for other catalytic reactions in the literature; for example see: (a) A. Gómez-Suárez, Y. Oonishi, A. R. Martin, S. V. C. Vummaleti, D. J. Nelson, D. B. Cordes, A. M. Z. Slawin, L. Cavallo, S. P. Nolan and A. Poater, *Chem. Eur. J.*, 2016, **22**, 1125–1132; (b) È. Casals-Cruaños, O. F. González-Belman, P. Besalú-Sala, D. J. Nelson and A. Poater, *Org. Biomol. Chem.*, 2017, **15**, 6416–6425.
- 20 As an example, our preliminary calculations concerning double hydroarylation of alkynes using furans and thiophenes in acetic acid (C. Luo, H. Yang, R. Mao, C. Lu and G. Cheng, *New J. Chem.*, 2015, **39**, 3417) show that these catalytic reactions are rationalized only if we invoke a binuclear mechanism similar to that outlined in Fig. 4. This is an ongoing project, details of which will appear elsewhere.
- 21 M. J. Frisch, G. W. Trucks, H. B. Schlegel, G. E. Scuseria, M. A. Robb, J. R. Cheeseman, G. Scalmani, V. Barone, B. Mennucci, G. A. Petersson, H. Nakatsuji, M. Caricato, X. Li, H. P. Hratchian, A. F. Izmaylov, J. Bloino, G. Zheng, J. L. Sonnenberg, M. Hada, M. Ehara, K. Toyota, R. Fukuda, J. Hasegawa, M. Ishida, T. Nakajima, Y. Honda, O. Kitao, H. Nakai, T. Vreven, J. A. Montgomery, Jr., J. E. Peralta, F. Ogliaro, M. Bearpark, J. J. Heyd, E. Brothers, K. N. Kudin, V. N. Staroverov, R. Kobayashi, J. Normand, K. Raghavachari, A. Rendell, J. C. Burant, S. S. Iyengar, J. Tomasi, M. Cossi, N. Rega, J. M. Millam, M. Klene, J. E. Knox, J. B. Cross, V. Bakken, C. Adamo, J. Jaramillo, R. Gomperts, R. E. Stratmann, O. Yazyev, A. J. Austin, R. Cammi, C. Pomelli, J. W. Ochterski, R. L. Martin, K. Morokuma, V. G. Zakrzewski, G. A. Voth, P. Salvador, J. J. Dannenberg, S. Dapprich, A. D. Daniels, O. Farkas, J. B. Foresman, J. V. Ortiz, J. Cioslowski and D. J. Fox, Gaussian 09, Revision D.01; Gaussian, Inc.: Wallingford, CT, 2009
- 22 (a) C. T. Lee, W. T. Yang and R. G. Parr, *Phys. Rev. B.*, 1988, **37**, 785; (b) B. Miehlich, A. Savin, H. Stoll and H. Preuss, *Chem. Phys. Lett.*, 1989, **157**, 200; (c) A. D. Becke, *J. Chem. Phys.*, 1993, **98**, 5648
- 23 (a) V. Barone and M. Cossi, *J. Phys. Chem. A.*, 1998, **102**, 1995; (b) M. Cossi, N. Rega, G. Scalmani and V. Barone, *J. Comput. Chem.*, 2003, **24**, 669
- 24 (a) P. J. Hay and W. R. Wadt, *J. Chem. Phys.*, 1985, **82**, 270; (b) W. R. Wadt and P. J. Hay, *J. Chem. Phys.*, 1985, **82**, 284
- 25 P. C. Hariharan and J. A. Pople, *Theor. Chim. Acta.*, 1973, **28**, 213
- 26 A. W. Ehlers, M. Böhme, S. Dapprich, A. Gobbi, A. Höllwarth, V. Jonas, K. F. Köhler, R. Stegmann, A. Veldkamp and G. Frenking, *Chem. Phys. Lett.*, 1993, **208**, 111
- 27 (a) K. Fukui, *J. Phys. Chem.*, 1970, **74**, 4161; (b) K. Fukui, *Acc. Chem. Res.*, 1981, **14**, 363
- 28 S. Grimme, J. Antony, S. Ehrlich and H. Krieg, *J. Chem. Phys.* 2010, **132**, 154104.
- 29 F. Weigend, F. Furche and R. Ahlrichs, *J. Chem. Phys.*, 2003, **119**, 12753.
- 30 For references related to the M06 functional see (a) Y. Zhao and D. G. Truhlar, *Theor. Chem. Acc.*, 2008, **120**, 215; (b) Y. Zhao and D. G. Truhlar, *Acc. Chem. Res.*, 2008, **41**, 157.
- 31 For references related to the B97D functional see (a) S. Grimme, *J. Comput. Chem.*, 2006, **27**, 1787; (b) A. D. Becke, *J. Chem. Phys.*, 1997, **107**, 8554.
- 32 E. D. Glendening, J. K. Badenhoop, A. E. Reed, J. E. Carpenter, J. A. Bohmann, C. M. Morales, C. R. Landis and F. Weinhold, Natural Bond Order 6.0; Theoretical Chemistry Institute, University of Wisconsin, Madison, WI, 2013; <http://nbo6.chem.wisc.edu>
- 33 E. D. Glendening, C. R. Landis and F. Weinhold, *J. Comput. Chem.*, 2013, **34**, 1429.